JOURNAL OF Applied Polymer SCIENCE

Balancing mechanical properties and processability for devulcanized ground tire rubber using industrially sized single-screw extruder

Xiao-Long Lv,[1] Han-Xiong Huang,[1] Bai-Yuan Lv[2]

[1]Lab for Micro Molding and Polymer Rheology, Department of Industrial Equipment and Control Engineering, South China University of Technology, Guangzhou 510640, People's Republic of China

[2]Institute for Polymer Processing Machinery, School of Mechanical Engineering, Qingdao University of Science and Technology, Qingdao 266061, People's Republic of China

Correspondence to: H.-X. Huang (E-mail: mmhuang@scut.edu.cn)

ABSTRACT: Devulcanized ground tire rubber (DGTR) samples were produced using an independently developed industrially sized single-screw extruder. The DGTR was further revulcanized to produce revulcanized DGTR (RDGTR) samples. The structure and properties of the produced samples were investigated via tests and characterization of sol fraction, crosslink density, Fourier transform infrared spectroscopy spectra, X-ray photoelectron spectroscopy spectra, Mooney viscosity, curing characteristics, dynamic rheology, tensile properties, and surface morphology. The results demonstrate that the extruder can effectively break up crosslinked structure of ground tire rubber to achieve high devulcanization level (characterized by sol fraction and crosslink density), which is mainly associated with its moderate shear strength. The balance between mechanical properties and processability for the DGTR samples was analyzed. Lower ratios of main-chain to crosslink scission and good processability (mainly characterized by modest Mooney viscosity) for the DGTR samples, and high tensile strengths and elongations at break for the RDGTR samples are obtained via appropriately combining the barrel temperature and screw speed. High quality DGTR sample with tensile strength and elongations at break of up to 11 MPa and 370%, respectively, is prepared under the conditions used in this work. © 2016 Wiley Periodicals, Inc. J. Appl. Polym. Sci. **2016**, *133*, 43761.

KEYWORDS: extrusion; properties and characterization; rubber; recycling; structure–property relations

Received 27 January 2016; accepted 10 April 2016

DOI: 10.1002/app.43761

INTRODUCTION

Significantly grown amounts of waste rubbers are produced worldwide, which mainly results from fast development of automotive industry. Recycling waste rubbers can settle environmental problem and provide reclaimed rubber, and so has attracted much attention from both industry and academia. Rubber recovery, however, is not an easy matter because vulcanized rubbers have three-dimensional crosslinked structure.[1]

Enormous efforts have been made to develop a number of techniques to devulcanize waste rubbers especially ground tire rubber (GTR). These techniques mainly include thermomechnical,[2,3] mechanochemical,[4,5] microwave,[6–8] ultrasonic,[9–11] microbial,[12–14] and solid state shear pulverization[15,16] methods. Among these devulcanization methods, thermomechnical continuous devulcanization via shearing has a largely industrialized potential.[17] Thermomechnical continuous devulcanization is mainly realized by using twin-screw extruders.[17–30] In most of these works, effects of extruder screw configuration and processing conditions (screw speed, barrel temperature, feeding rate) on the devulcanization efficiency and the structure and performance of devulcanized rubber were investigated, and possible devulcanizing mechanism was analyzed. The results demonstrate that higher devulcanization efficiency can be achieved under appropriate conditions.

Recently, Zhang *et al.*[1] investigated and compared the structure and properties of the reclaimed rubbers prepared by using four different reclaiming methods. The results showed that the reclaiming process by twin-screw extruder is dominated by main chain scission due to strong shear force and high temperature, which results in very low Mooney viscosities for the reclaimed rubbers and lower mechanical properties for the revulcanized reclaimed rubbers. Moreover, the recommended reclaiming method would be a process under oxygen-free atmosphere, without severe shear force and at relative low temperature. As well-known that single-screw extruder exerts lower shear force on the materials than twin-screw extruder. Actually, single-screw extruders were employed in ultrasonic devulcanization by Isayev *et al.*[9,10] and in solid state shear pulverization by Bilgili *et al.*[15] Recently, an industrially sized single-screw extruder specially used for devulcanizing waste rubbers was developed in our research group.

Figure 1. Schematics for screw of industrially sized single-screw extruder used in this work.

For the aforementioned reasons, the developed single-screw extruder was used to devulcanize GTR in this work. Shear, temperature, and residence time are main processing parameters affecting the devulcanization degree in devulcanization process using an extruder. So the influences of barrel temperature and screw speed of the single-screw extruder on the structure and properties of the devulcanize GTR (DGTR) were investigated via systematic tests and characterization. The balance between mechanical properties and processability for the DGTR was analyzed.

EXPERIMENTAL

Equipment and Materials

A large-sized single-screw extruder was developed to be specially used for devulcanization of ground rubbers continuously and industrially in our research group. The extruder is equipped with a screw (schematically depicted in Figure 1) having a diameter of 120 mm, length-to-diameter ratio of 40, and compression ratio of 1.7. The screw is divided into six zones, namely, one feeding, two conveying, two shearing, and one pumping zones. Flights in conveying zones 1 especially 2 have a smaller helix angle than that in the feeding zone. A barrier flight is introduced in shearing zones 1 and 2. The barrier flight has a larger helix angle and clearance than the main flight. The shear strength of the extruder screw is mainly dominated by the clearance of the barrier flight. Compounded stocks can be exposed to moderate shear force and more uniform temperature field when flowing across the barrier flight. Alternately arranged conveying and shearing zones are beneficial for simultaneous improvement of conveying and devulcanizing of the compounded stocks.

The GTR powder used in this work was prepared from recycled truck tires. Its average particle size was about 1 mm. Reclaiming agents, including aromatic oil, rosin and activator (B450), and curing agents, including accelerator (NS), zinc oxide (ZnO), sulfur and stearic acid, all were commercially available.

Sample Preparation

The GTR powder (100 phr) and reclaiming agents (aromatic oil 10 phr, rosin 1.2 phr, and activator 0.3 phr) were dry-mixed, and the mixture was then fed into the hopper of the single-screw extruder. DGTR samples were prepared under five different barrel temperatures (230–270 °C in step of 10 °C) at 30 rpm screw speed and different five screw speeds (15–35 rpm in step of 5 rpm) at 250 °C barrel temperature.

The as-extruded DGTR samples were collected for further revulcanizing to produce revulcanized DGTR (RDGTR) samples according to the formulation suggested by Standard GB/T 13460–2008 (China) (DGTR 300 g, accelerator 2.4 g, ZnO 7.5 g, sulfur 3.5 g, and stearic acid 1.0 g). Specifically, the DGTR sample and curing agents were compounded in a two roll mill. The compounded stock was then placed in a mold and pressed by using a platen press at 16 MPa and 145 °C to prepare RDGTR samples with a thickness of about 2 mm. Dumbbell-shaped specimens were punched out from the RDGTR samples.

Tests and Characterization

Sol Fraction Measurements. The sol fraction of the DGTR samples was measured using Soxhlet extraction method. The sample wrapped with wire mesh was put into Soxhlet extractor to be extracted with acetone for 12 h. The residue was dried for 6 h at 60 °C in a vacuum oven to a constant weight m_1. The dried residue was further extracted with toluene for 24 h, and the residue was dried for 8 h at 60 °C in a vacuum oven to a constant weight m_2. The sol fraction was calculated using the following equation:

$$\text{Sol fraction} = \frac{m_1 - m_2}{m_1} \quad (1)$$

Crosslink Density Measurements. The crosslink density of the DGTR samples was determined by a swelling technique using toluene as a solvent. Small pieces of specimens cut from the DGTR samples were immersed in toluene for 72 h at room temperature. The Flory–Rehner equation[31] with Kraus correction[32] was used to calculate the crosslink density.

Fourier Transform Infrared Spectroscopy (FTIR). FTIR absorption spectra of the DGTR samples were recorded with a FTIR spectrometer (Vertex 70, Bruker, Germany). The scanning range was 4000–400 cm^{-1} with a resolution of 4 cm^{-1}.

X-ray Photoelectron Spectroscopy (XPS). XPS spectra of the DGTR samples were recorded with an XPS spectrometer (ESCALAB250, Thermo Scientific, USA). Binding energies were corrected to the carbon 1s peak locating at 285.0 eV.

Mooney Viscosity Measurements. The Mooney viscosity of the DGTR samples was measured using a Mooney viscometer (JMN-III, Yangzhou Jingyi Test Machine, China) according to Standard GB/T 1232.1–2000 (China).

Curing Characteristic and Dynamic Rheological Measurements. The DGTR sample and curing agents were compounded in a two roll mill using the same formulation to that in preparing the aforementioned RDGTR samples. A disk specimen cut from the compounded stock was placed in a rubber process analyzer (RPA2000, Alpha, USA). The measurements were preformed first at a temperature of 60 °C to give the dynamic rheological properties for the DGTR sample and subsequently at 160 °C to give the curing characteristics for the DGTR sample and the dynamic rheological properties for the RDGTR sample. The frequency was set at 1.7 Hz in the measurement process.

Tensile Testing. Tensile tests were carried out on the dumbbell-shaped RDGTR specimens using a testing machine (JDL-5000, Yangzhou Jingyi Test Machine, China) at room temperature and

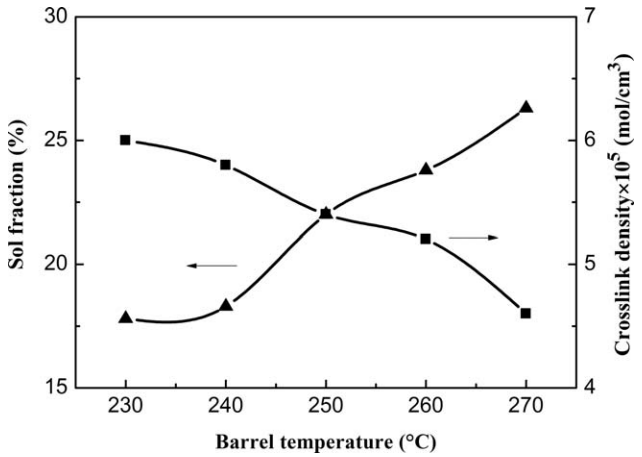

Figure 2. Sol fraction and crosslink density curves for DGTR samples versus barrel temperature.

a crosshead speed of 500 mm/min according to Standard GB/T 528–2009 (China). Each experiment was repeated for five times.

Scanning Electron Microscopy (SEM) Observation. The surfaces of the GTR powder and DGTR samples and the cryofractured surface of the RDGTR samples were sputtered with gold and then observed by using an SEM (JSM-6700F, JEOL, Japan).

RESULTS AND DISCUSSION

Effect of Barrel Temperature

The effect of the barrel temperature (230–270 °C) used in devulcanizing the GTR by the extruder on the structure and properties of the DGTR samples was investigated at a fixed screw speed of 30 rpm.

Devulcanization Level

The devulcanization level for devulcanizates can be characterized by sol fraction or crosslink density. They can reflect the characteristics of the structure in devulcanizates indirectly. Figure 2 illustrates the sol fraction and crosslink density curves for the DGTR samples versus the barrel temperature. It is apparent that as raising the barrel temperature from 230 to 270 °C, the sol fraction increases slightly at first and then obviously, whereas the crosslink density decreases monotonously.

Scission of crosslink bonds is usually accompanied by main-chain scission during devulcanization of ground rubbers. Here Horikx's theory[33] was used to determine the ratio of main-chain to crosslink scissions in the prepared DGTR samples. According to Horikx's theory, a theoretical relationship between the sol fraction and the relative decrease in the crosslink density for the DGTR samples prepared under different barrel temperatures is obtained and shown in Figure 3, in which V_i and V_f are the crosslink densities of the GTR powder and DGTR samples. The devulcanization process is more dominated by scission of the crosslink bonds [mainly sulfur–sulfur (S—S) and carbon–sulfur (C—S) bonds] when data points are located near the crosslink scission curve.

The fraction of sol component existing in devulcanizates can be used to characterize devulcanization efficiency or rubber network scission degree.[17] Generally, the higher the sol fraction is, the more efficient the devulcanization is. The sol fraction for the GTR powder used in this work is measured to be about 5.1%. Increased sol fractions are obtained for the prepared DGTR samples (shown in Figure 2), which confirms that the crosslinked structure in the GTR is effectively broken by using the single-screw extruder developed in this work. As raising the barrel temperature, on the one hand, the sol fraction increases and the crosslink density decreases, suggesting the scission of more crosslink bonds and also main chains in devulcanizing the GTR; on the other hand, the data points shown in Figure 3 move away from the crosslink scission towards main-chain scission curves gradually, meaning increased ratio of main-chain to crosslink scission. That is, higher sol fractions in the DGTR samples at higher barrel temperatures are gained at the expense of severer main-chain scission. This is attributed to more heat absorption for the GTR powder when it is conveyed and sheared along the screw at higher barrel temperatures.

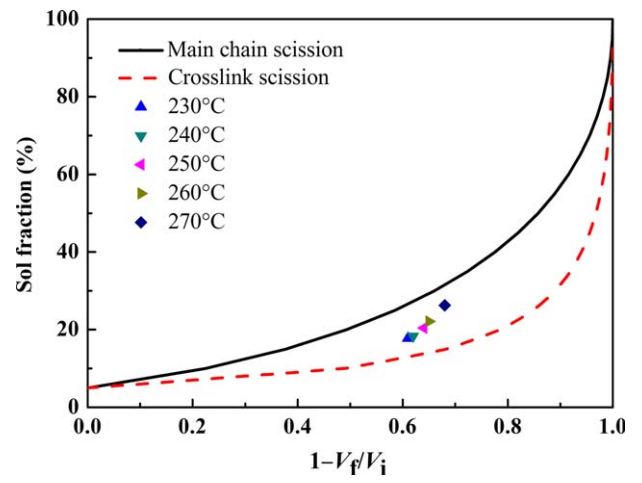

Figure 3. Sol fraction versus relative decrease in crosslink density for DGTR samples prepared at different barrel temperatures. [Color figure can be viewed in the online issue, which is available at wileyonlinelibrary.com.]

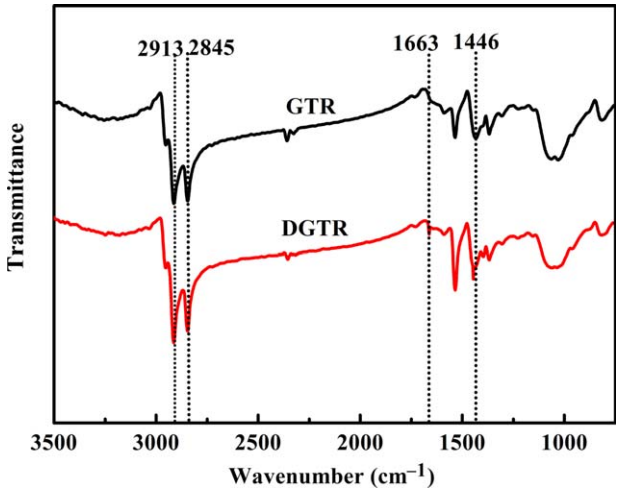

Figure 4. FTIR spectra for GTR powder and DGTR sample prepared at barrel temperature of 250 °C. [Color figure can be viewed in the online issue, which is available at wileyonlinelibrary.com.]

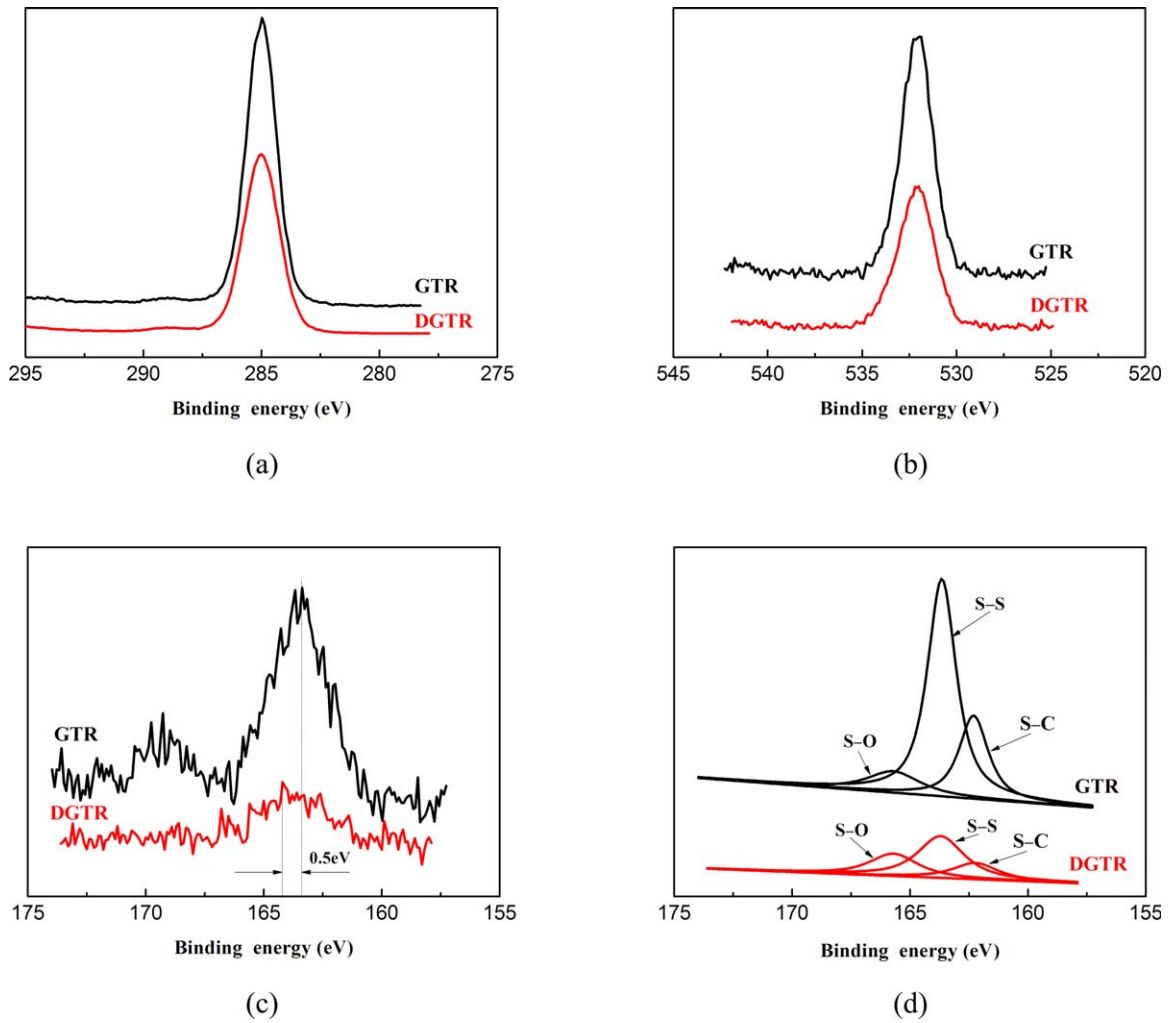

Figure 5. (a) C1s, (b) O1s, and (c) S2p core spectra and (d) structural changes in sulfide bonds on surfaces for GTR powder and DGTR sample prepared at barrel temperature of 250 °C. [Color figure can be viewed in the online issue, which is available at wileyonlinelibrary.com.]

Characterization of Devulcanization

Figure 4 shows the FTIR absorbance spectra for the GTR powder used in this work and the DGTR sample prepared at a barrel temperature of 250 °C. Both of them exhibit absorption peaks at 1446, 1663, 2845, and 2913 cm^{-1}, which are all characteristic absorption peaks of nature rubber (*cis*-polyisoprene). The absorption peaks at 1446 and 1663 cm^{-1} are assigned to the bending vibration of methylene group ($–CH_2–$) and the stretching vibration of carbon–carbon double bond (C═C), respectively. The peaks at 2845 and 2913 cm^{-1} are assigned to the saturated carbon–hydrogen bond (C—H). As can be seen in Figure 4, both DGTR sample and GTR powder exhibit similar FTIR spectra. The main difference lies in somewhat strengthened absorption peaks at 1446 and 1663 cm^{-1} for the former. This may be attributed to partial breakage of C—S crosslink bond and so formation of the $–CH_2–$ group and the C═C

Table I. Surface Element Contents for GTR Powder and DGTR Sample Prepared at Barrel Temperature of 250 °C

Element	C (%)	O (%)	S (%)
GTR	93.65	5.75	0.60
DGTR	94.39	5.34	0.27

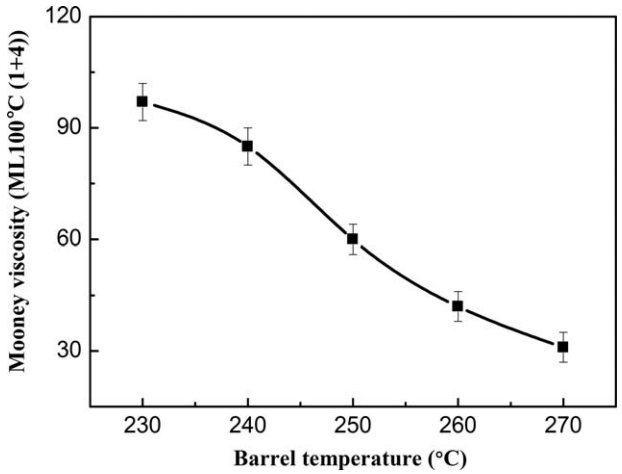

Figure 6. Mooney viscosity curve for DGTR samples versus barrel temperature.

Table II. Curing Characteristics for DGTR Samples Prepared at Different Barrel Temperatures

Barrel temperature (°C)	M_{min} (dNm)	M_{max} (dNm)	ΔM	t_{10} (min)	t_{90} (min)
230	1.58	10.89	9.31	1.9	4.0
240	1.43	10.72	9.29	2.0	4.0
250	1.08	9.82	8.74	2.0	4.0
260	0.83	8.98	8.15	2.0	4.1
270	0.61	7.76	7.15	2.0	4.1

bonds at the main chain under the coupling effects of the shear force, heat and reclaiming agents during devulcanization in the developed single-screw extruder. The S—S bond is lower than the C—S bond in bond energy, so it may be expected that partial S—S bonds are also broken in the case of the C—S bond breakage.

XPS analyses were employed to determine the contents and bonding states of C, O, and S elements for the GTR powder and the DGTR sample prepared at a barrel temperature of 250 °C. Figure 5 shows the C1s, O1s, and S2p core spectra and the structural changes in sulfide bonds on the surfaces for the GTR powder and the DGTR sample, whereas Table I lists the surface element contents. As can be seen, the DGTR sample exhibits almost unchanged C and O peaks as compared to the GTR powder [Figure 5(a,b)]. The S2p core spectra demonstrate that S peak is shifted about 0.5 eV to a high binding energy [Figure 5(c)] and both S—C bond at 162.3 eV and S—S bond at 163.7 eV are obviously reduced [Figure 5(d)] for the DGTR sample. It is obvious from Table I, the C and O contents almost remain unchanged, whereas the S content is substantially lowered. From the foregoing, partial S—C and S—S bonds in the GTR are broken by the extruder.

Mooney Viscosity

Mooney viscosity of devulcanizate is related to its structure. Figure 6 displays the Mooney viscosity curve of the DGTR samples versus the barrel temperature. As can be seen, the Mooney viscosity decreases gradually with raising barrel temperature, which exhibits opposite tendency of the sol fraction with the barrel temperature (Figure 2). This is associated with the plasticization effect of the sol fractions with low molecular weight.

Curing Characteristics

The curing characteristics of the DGTR samples, determined at 160 °C, are presented in Table II. As can be seen, both minimum and maximum torques (M_{min} and M_{max}) of the DGTR samples decrease with raising barrel temperature. Comparing Table II and Figure 6 demonstrates that both M_{min} and Mooney viscosity exhibit very similar tendency with the barrel temperature, which is because the M_{min} is a measure of the stock viscosity of devulcanizate.[1] The ΔM, which is the difference between values of the M_{max} and M_{min}, is related to the crosslink density. The curing agents are more apt to disperse in the sol part than to pass into the crosslinked gel part during devulcanization.[1] Accordingly, higher contents of sol parts with short molecular chains result in more difficult revulcanization for the DGTR samples containing sol and gel parts. Thus, the decrease in the ΔM with raising barrel temperature is attributed to the decreased crosslinking density (as shown in Figure 2). It can be also seen from Table II that all the DGTR samples exhibit almost the same values of the scorch time (t_{10}) and optimum cure time (t_{90}).

Mechanical and Rheological Properties

Figure 7 illustrates the tensile strength and elongation at break curves determined for the RDGTR samples versus the barrel temperature. It is clear that both of them first reduce modestly and then largely with raising barrel temperature. In fact, the mechanical properties of devulcanizate are determined principally by its devulcanization level or structure. Largely reduced mechanical properties for the RDGTR samples prepared at the barrel temperatures higher than 250 °C are explained as follows. Devulcanizate is mainly composed of the sol part resulting from main-chain and crosslink scissions and the gel part with a crosslink network. For the DGTR samples prepared at higher barrel temperatures, higher sol fractions suggest some severer main-chain scission (Figures 2 and 3); moreover, the main chains in the gel parts are more severely broken (Figure 2), which results in weaker gel structure with higher amounts of short molecular chains and so more inefficient revulcanization in preparing the RDGTR samples.

Oscillatory shear measurements with the rubber process analyzer at 60 °C and subsequently at 160 °C give the dynamic rheological properties for the DGTR samples and corresponding RDGTR samples, respectively. Figure 8 displays the storage modulus (G') and loss tangent (tan δ) curves versus strain for both samples. The results demonstrate that both samples exhibit gradually decreased G' with raising barrel temperature. The crosslink rubber network structure and carbon black–rubber network structure in devulcanizate play an important role on the values of its G'. Raising barrel temperature causes enhanced broken extent of the crosslinked structure in the GTR and decreased crosslink densities for the DGTR samples (shown in Figure 2), leading to the aforementioned gradual decrease of the G'. The tan δ exhibits a small increase with raising barrel

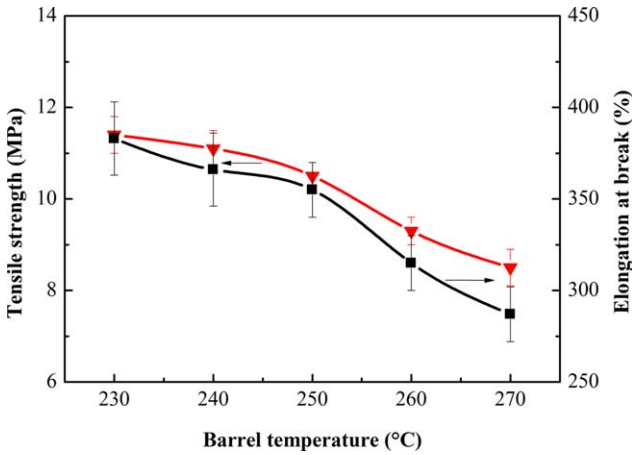

Figure 7. Tensile strength and elongation at break curves for RDGTR samples versus barrel temperature. [Color figure can be viewed in the online issue, which is available at wileyonlinelibrary.com.]

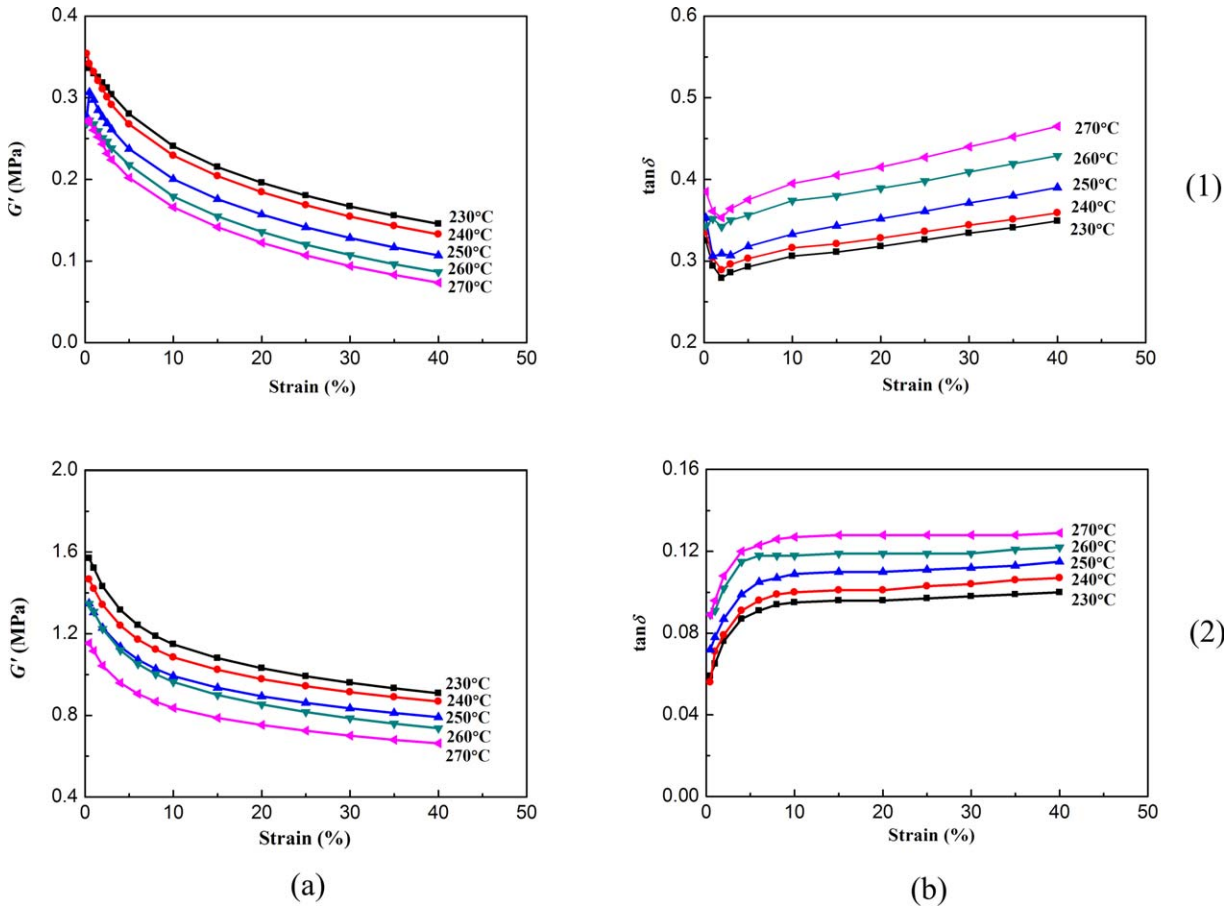

Figure 8. Strain dependence of (a) storage modulus (G') and (b) loss factor (tan δ) for (1) DGTR samples prepared at different barrel temperatures and (2) corresponding RDGTR samples. [Color figure can be viewed in the online issue, which is available at wileyonlinelibrary.com.]

temperature for both samples. As expected, the RDGTR samples exhibit obviously higher G' and lower tan δ than corresponding DGTR samples.

Balance between Mechanical Properties and Processability

Mechanical properties and processability are two important indicators for devulcanizates. The tensile strengths and elongations at break for the RDGTR samples decrease with raising barrel temperatures (Figure 7). The processability or flowability of devulcanizate is usually determined by its Mooney viscosity or M_{min} measured during curing. Both Mooney viscosity (Figure 6) and M_{min} (Table II) decrease with raising barrel temperature. That is, the mechanical properties and processability exhibit contrary tendency with the barrel temperature. So for balanced mechanical properties and processability of the DGTR samples, appropriate barrel temperatures should be set to break the crosslinked structure of the GTR to a certain extent but still maintain sufficient macromolecular chains for a certain degree of plasticity and deformability.

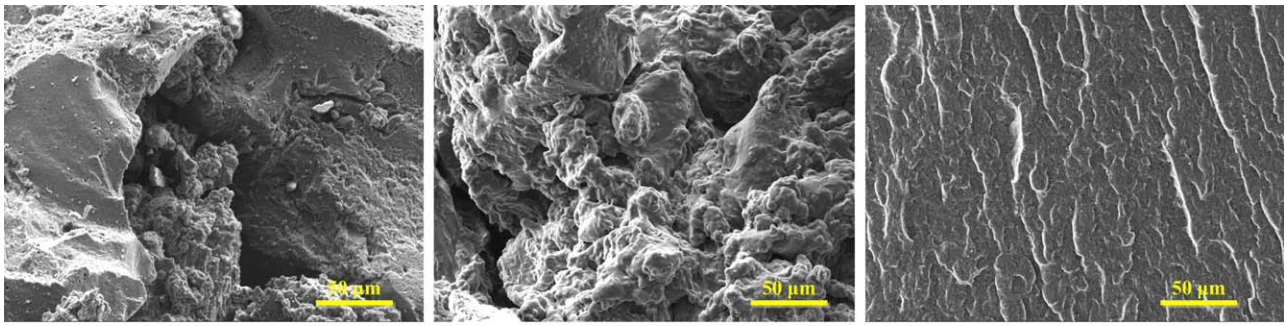

Figure 9. SEM micrographs of surfaces of (a) GTR powder and (b) DGTR sample prepared at barrel temperature of 250 °C and (c) cryofractured surface of corresponding RDGTR sample. [Color figure can be viewed in the online issue, which is available at wileyonlinelibrary.com.]

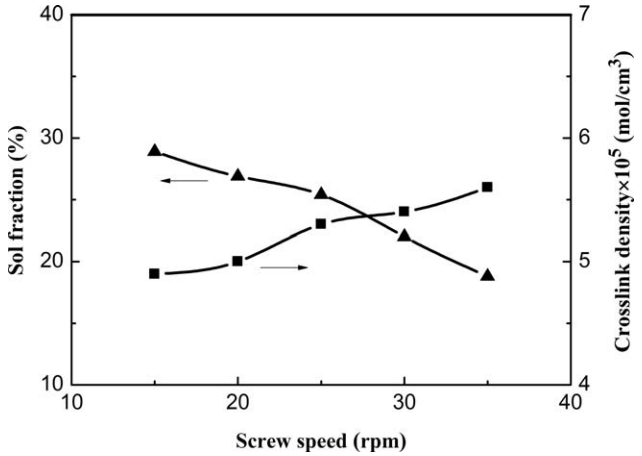

Figure 10. Sol fraction and crosslink density curves for DGTR samples versus screw speed.

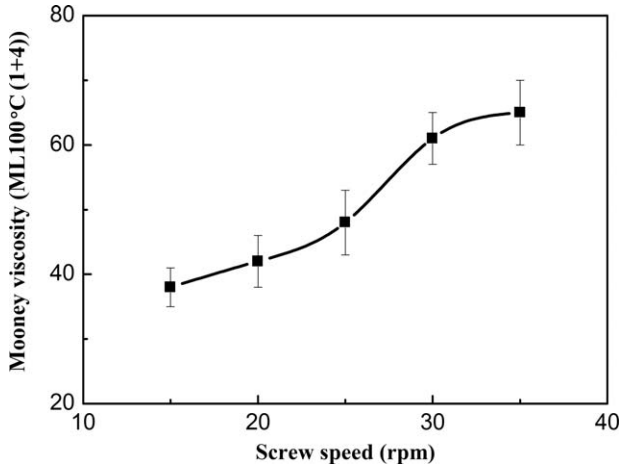

Figure 12. Mooney viscosity curve for DGTR samples versus screw speed.

According to Standard GB/T 13460–2008 (China), for high quality devulcanizates reclaimed from truck tires, the tensile strength should be higher than 9.0 MPa and the Mooney viscosity should be lower than 80 ML 100 °C (1 + 4). Combining Figures 6 and 7 demonstrates that the barrel temperatures should be set at 242–263 °C, at which the DGTR samples with balanced tensile strength and processability or with satisfied quality can be prepared.

Surface Morphology

Figure 9 displays the SEM micrographs of the surfaces of the GTR powder and the DGTR sample prepared at a barrel temperature of 250 °C and the cryofractured surface of the corresponding RDGTR sample. As can be seen, obviously different morphologies appear on the three surfaces, which further confirms the recovery of plasticity in the DGTR sample and the distinctly vulcanized structure in the RDGTR sample.

Effect of Screw Speed

From the foregoing, barrel temperatures of 242–263 °C are appropriate for balancing the mechanical properties and processability of the DGTR samples. So the following investigation is carried out at a barrel temperature of 250 °C in terms of the effect of the screw speed (15–35 rpm) on the structure and properties of the DGTR samples.

Shown in Figure 10 are the sol fraction and crosslink density curves for the DGTR samples versus the screw speed. One finds that the sol fraction decreases and the crosslink density increases with increasing screw speed. Figure 11 is the sol fraction versus the relative decrease in the crosslink density for the DGTR samples prepared under different screw speeds. As can be seen, the data points move away from the main-chain scission towards crosslink scission curves gradually with increasing screw speed. Figure 12 illustrates the Mooney viscosity against the screw speed for the DGTR samples. Table III lists the curing characteristics of the DGTR samples determined at 160 °C. Figure 13 displays the tensile strength and elongation at break curves versus the screw speed for the RDGTR samples. Figure 14 illustrates the strain dependence of the G' and tan δ for both DGTR and RDGTR samples. As can be seen, there is not much difference among the values of the tan δ for the samples prepared at different screw speeds.

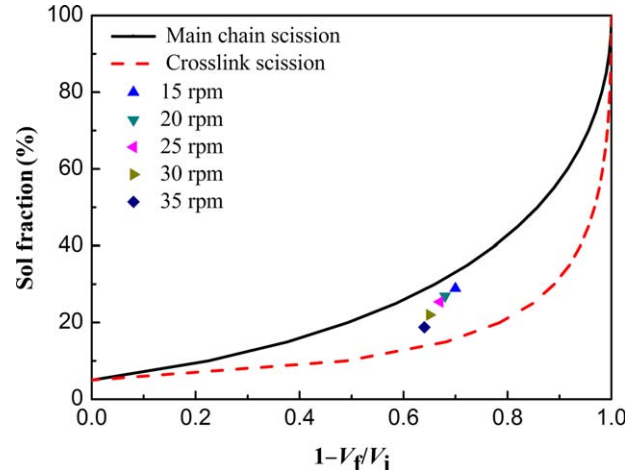

Figure 11. Sol fraction versus relative decrease in crosslink density for DGTR samples prepared at different screw speeds. [Color figure can be viewed in the online issue, which is available at wileyonlinelibrary.com.]

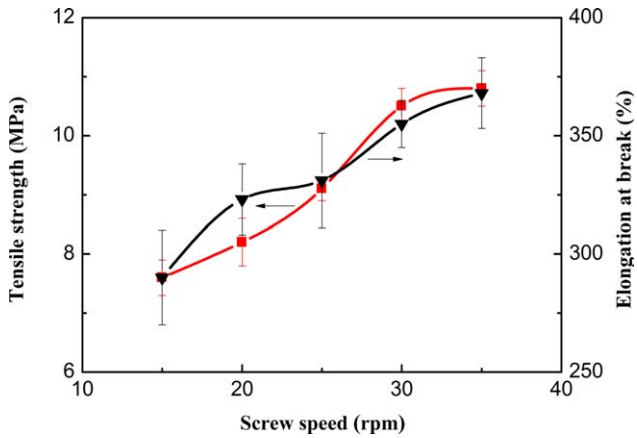

Figure 13. Tensile strength and elongation at break curves for RDGTR samples versus screw speed. [Color figure can be viewed in the online issue, which is available at wileyonlinelibrary.com.]

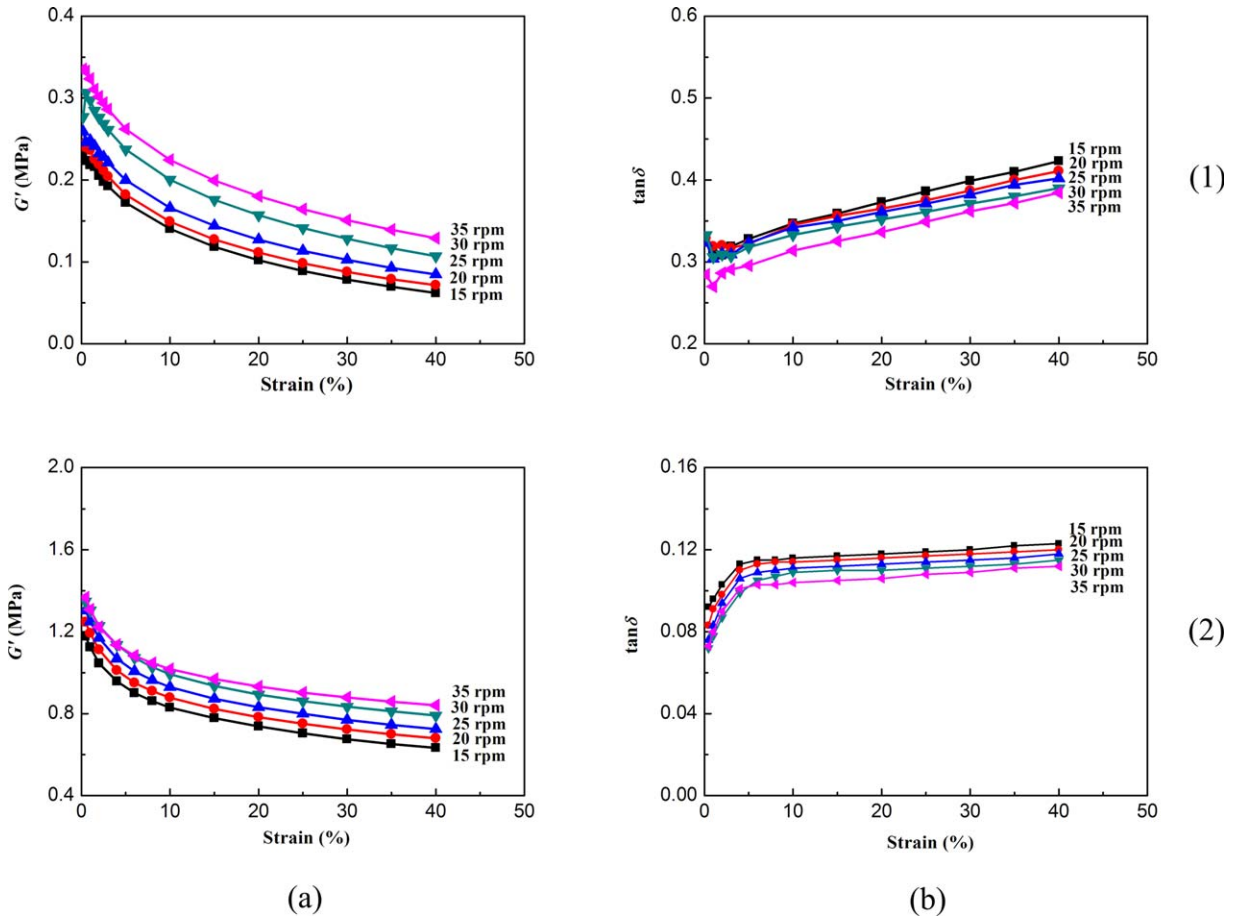

Figure 14. Strain dependence of (a) storage modulus (G') and (b) loss factor (tan δ) for (1) DGTR samples prepared at different screw speeds and (2) corresponding RDGTR samples. [Color figure can be viewed in the online issue, which is available at wileyonlinelibrary.com.]

It can be found from comparatively analyzing Figures 10–14 and Table III that the sol fraction decreases modestly and so the Mooney viscosity, M_{min}, tensile strength, and G' increase modestly as increasing the screw speed from 15 to 25 rpm, whereas the variation tendencies are relatively large as increasing the screw speed from 25 to 35 rpm. This can be explained as follows. Generally, increasing the screw speed plays a dual role in devulcanizing waste rubbers via increasing the shear force and shortening the residence time of stocks in an extruder.[26] The former effect increases the sol fraction of devulcanizate, whereas the latter effect decreases the sol fraction. Considering that the extruder used is the single-screw one and the screw speeds are lower in this work, the residence time instead of shear force dominates the devulcanization process. Thus, the sol fraction decreases with increasing screw speed. At low screw speeds (15–25 rpm), the viscosity of the compounded stocks in the extruder is high due to lower shear force exerted on the stocks, which additionally extends their residence time. So modest decreasing tendency appears for the sol fraction (Figure 10). Moreover, longer residence time increases the heat absorption for the stocks at higher barrel temperature (250 °C), which results in higher ratio of main-chain to crosslink scission (Figure 11) and so corresponding properties (Figures 12–14). In order to achieve the aforementioned high quality DGTR samples, that is, tensile strengths of above 9.0 MPa and Mooney viscosities of below 80 ML 100 °C (1 + 4), the screw speeds should be above 25 rpm in this work.

Table III. Curing Characteristics for DGTR Samples Prepared at Different Screw Speeds

Screw speed (rpm)	M_{min} (dNm)	M_{max} (dNm)	ΔM	t_{10} (min)	t_{90} (min)
15	0.66	7.88	7.22	2.1	4.1
20	0.72	8.34	7.62	2.1	4.1
25	0.86	9.03	8.17	2.1	4.1
30	1.08	9.82	8.74	2.0	4.0
35	1.25	10.37	9.12	2.0	4.0

CONCLUSIONS

Large-sized single-screw extruder developed in our group was applied for devulcanizing the GTR in the current work. The GTR is effectively devulcanized by using the extruder, which is confirmed by the increased sol fractions and decreased crosslinking density in the prepared DGTR samples. The FTIR and XPS analyses and the relationship between the sol fraction and the relative decrease in the crosslink density reveal that partial

crosslink bonds (mainly S–S and C–S bonds) in the GTR are broken. The devulcanization process can be more dominated by scission of the crosslink bonds through adjusting the barrel temperature and/or screw speed of the extruder. Measuring and analyzing the Mooney viscosity, curing characteristics, and dynamic rheological properties for the DGTR samples and the dynamic rheological properties, tensile strength, and elongation at break for the RDGTR samples demonstrates that the DGTR samples having both high quality and good processability can be produced via appropriately combining the barrel temperature and screw speed.

ACKNOWLEDGMENTS

Financial support provided by Guangdong Provincial Natural Science Foundation is gratefully acknowledged.

REFERENCES

1. Shi, J. W.; Jiang, K.; Ren, D. Y.; Zou, H.; Wang, Y.; Lv, X. J.; Zhang, L. Q. *J. Appl. Polym. Sci.* **2013**, *129*, 999.
2. Hershaft, A. *Environ. Sci. Technol.* **1972**, *6*, 412.
3. Manuel, H. J.; Dierkes, W. *Rapra. Rev. Rep.* **1999**, *9*, 99.
4. Sekhar, B. C.; Subramaniam, A. Eur. Pat. EP0,748,837 (**1996**).
5. Jana, G. K.; Das, C. K. *Macromol. Res.* **2005**, *13*, 30.
6. Novotny, D. S.; Marsh, R. L.; Masters, F. C.; Tally, D. N. U.S. Patent 4,104,205 (**1978**).
7. Fix, S. R. *Elastomerics* **1980**, *112*, 38.
8. Scuracchio, C. H.; Waki, D. A.; Silva, M. L. C. P. *J. Therm. Anal. Calorim.* **2007**, *87*, 893.
9. Isayev, A. I.; Chen, J.; Tuchachinsky, A. *Rubber Chem. Technol.* **1995**, *68*, 267.
10. Yun, J.; Isayev, A. I.; Kim, S. H.; Tapale, M. *J. Appl. Polym. Sci.* **2003**, *88*, 434.
11. Zhu, S. H.; Alexer, P.; Costas, T. *J. Appl. Polym. Sci.* **2012**, *124*, 2062.
12. Fliermans, C. B. U.S. Patent 6,479,558 (**2002**).
13. Jiang, G. M.; Zhao, S. H.; Luo, J. Y.; Wang, Y. Q.; Yu, W. Y.; Zhang, C. R. *J. Appl. Polym. Sci.* **2010**, *116*, 2768.
14. Yao, C.; Zhao, S. H.; Wang, Y. Q.; Wang, B. W.; Wei, M. L.; Hu, M. H. *Polym. Degrad. Stabil.* **2013**, *98*,
15. Bilgili, E.; Arastoopour, H.; Bernstein, B. *Rubber Chem. Technol.* **2000**, *73*, 340.
16. Wu, H. J.; Liang, M.; Lu, C. H. *J. Appl. Polym. Sci.* **2011**, *122*, 257.
17. Tao, G. L.; He, Q. H.; Xia, Y. P.; Jia, G. C.; Yang, H. C.; Ma, W. Z. *J. Appl. Polym. Sci.* **2013**, *129*, 2598.
18. Mouri, M.; Usuki, A.; Sato, N. U.S. Patent 5,672,630 (**1997**).
19. Izumoto, R.; Ohshima, N. U.S. Patent 6,335,377 (**2002**).
20. Mouri, M.; Okamoto, H.; Matsushita, M.; Honda, H.; Nakashima, K.; Takeushi, K.; Suzuki, Y.; Owaki, M. *Inter. Polym. Sci. Technol.* **2000**, *27*, 17.
21. Maridass, B.; Gupta, B. R. *Polym. Test.* **2004**, *23*, 377.
22. Maridass, B.; Gupta, B. R. *Polym. Compos.* **2008**, *29*, 1350.
23. Sutanto, P.; Picchioni, F.; Janssen, L. P. B. M. *J. Appl. Polym. Sci.* **2006**, *102*, 5028.
24. Sutanto, P.; Picchioni, F.; Janssen, L. P. B. M. *Chem. Eng. Sci.* **2006**, *61*, 7077.
25. Hamid, Y.; Mohammad, K.; Ismaeil, G.; Hamed, A.; Gholam Reza, B. *J. Vinyl. Addit. Techol.* **2011**, *17*, 64.
26. Shi, J. W.; Zou, H.; Ding, L. L.; Li, X. L.; Jiang, K.; Chen, T.; Zhang, X. D.; Zhang, L. Q.; Ren, D. Y. *Polym. Degrad. Stab.* **2014**, *99*, 166.
27. Formela, K.; Cysewska, M.; Haponiuk, J. T. *Polimery* **2014**, *59*, 170.
28. Formela, K.; Cysewska, M.; Haponiuk, J. T.; Stasiek, A. *Polimery* **2013**, *58*, 906.
29. Wang, X. J.; Shi, C. P.; Zhang, L.; Zhang, Y. C. *J. Appl. Polym. Sci.* **2013**, *130*, 1845
30. Si, H.; Chen, T. J.; Zhang, Y. C. *J. Appl. Polym. Sci.* **2013**, *128*, 2307.
31. Flory, P. J.; Rehner, J. *J. Chem. Phys.* **1943**, *11*, 521.
32. Kraus, G. *J. Appl. Polym. Sci.* **1963**, *7*, 861.
33. Horikx, M. M. *J. Polym. Sci.* **1956**, *19*, 445.

SGML and CITI Use Only
DO NOT PRINT